

# Exploring mechanisms of spatial segregation between body size groups within fish populations under environmental change

Hsiao-Hang Tao<sup>1</sup>, Chun-Wei Chang<sup>2</sup>, and Chih-hao Hsieh<sup>3</sup>

<sup>1</sup>National Taiwan University Institute of Oceanography

<sup>2</sup>National Taiwan University

<sup>3</sup>National Taiwan University

December 20, 2022

## Abstract

Ample evidence has indicated shifts in distribution of fish populations in response to environmental stress. However, most studies focused at the whole population scale. This neglects the spatial dynamics between groups of different body size (body size groups), that fundamentally shapes the spatial structure of a population. Here, we explored the mechanisms that modulate spatial dynamics of body size groups, and applied our analyses to three North Sea fish populations which experienced severe declines in biomass from 1977 to 2019: Atlantic cod (*Gadus morhua*), haddock (*Melanogrammus aeglefinus*), and whiting (*Merlangius merlangius*). All three populations exhibited strong declines in the overlapped area between body size groups in winter over 43 years, yet their mechanisms differed. These declines were either due to (1) different magnitudes of contraction of the distribution area of body size groups; and/or (2) different speeds and directions of spatial shift among various body size groups, both increasing spatial segregation within populations. These patterns were either associated with ocean warming, and/or declining population biomass, and such associations often varied according to distinct body size groups. Our analytical approach provides a powerful tool for identifying vulnerable populations under environmental stress and can be generalized to study a variety of size/age structured populations at various ecosystem types.

## 1 **Abstract**

2 Ample evidence has indicated shifts in distribution of fish populations in response  
3 to environmental stress. However, most studies focused at the whole population scale. This  
4 neglects the spatial dynamics between groups of different body size (body size groups), that  
5 fundamentally shapes the spatial structure of a population. Here, we explored the  
6 mechanisms that modulate spatial dynamics of body size groups, and applied our analyses  
7 to three North Sea fish populations which experienced severe declines in biomass from 1977  
8 to 2019: Atlantic cod (*Gadus morhua*), haddock (*Melanogrammus aeglefinus*), and whiting  
9 (*Merlangius merlangius*). All three populations exhibited strong declines in the overlapped  
10 area between body size groups in winter over 43 years, yet their mechanisms differed. These  
11 declines were either due to (1) different magnitudes of contraction of the distribution area  
12 of body size groups; and/or (2) different speeds and directions of spatial shift among various  
13 body size groups, both increasing spatial segregation within populations. These patterns  
14 were either associated with ocean warming, and/or declining population biomass, and such  
15 associations often varied according to distinct body size groups. Our analytical approach  
16 provides a powerful tool for identifying vulnerable populations under environmental stress  
17 and can be generalized to study a variety of size/age structured populations at various  
18 ecosystem types.

## 19 **Keywords**

20 biogeography, marine ecology, ocean warming, population spatial structure, population  
21 spatial shift.

## 22 **Introduction**

23 Many marine fish populations have undergone significant shifts in their spatial  
24 distributions over the past decades, largely related to ocean warming and declining  
25 population size (Perry et al. 2005, Sunday et al. 2015). Most of these studies focused at the  
26 whole population scale; however, several lines of evidence have suggested that the spatial  
27 shift varies in magnitude and direction for different body size groups within a population  
28 (hereafter, body size groups) (Bell et al. 2015, Barbeaux and Hollowed 2018, Frank et al.  
29 2018, Yang et al. 2019, Li et al. 2022). For instance, the distribution of the middle size  
30 groups of some fishes populations in the Eastern Bering Sea shifted at a greater speed in  
31 warm seasons, compared to groups of smaller or larger body sizes (Barbeaux and Hollowed  
32 2018). Another study across North Pacific, North Atlantic, and South Atlantic suggested  
33 that the distribution of large size groups within some fish populations shifted deeper, as a  
34 result of size-selective fishing at shallower water (Frank et al. 2018). These size-dependent  
35 shifts in distribution are likely to reduce overlapped areas between body size groups, that is,  
36 increase the spatial segregation within populations. However, temporal changes in spatial  
37 segregation (i.e., overlapped area) between body size groups have not been quantified for  
38 real-world populations, despite earlier efforts from theoretical approaches (Hughes and  
39 Grand 2000).

40 Changes in spatial segregation between body size groups of a population have  
41 various consequences on population dynamics. On one hand, a population with high spatial  
42 segregation between body size groups can reduce the stress from predation and competition.  
43 On the other hand, a population with highly segregated size group is more vulnerable to  
44 local perturbations. These perturbations include size-selective fishing, size-selective  
45 predation, or unfavorable habitat conditions for certain body size groups (Hsieh et al. 2010b).  
46 These perturbations can change the abundance of certain body size groups, which in turn  
47 alter the demographic structure and spatial structure of the population (Tao et al. 2021).

48 More generally, changes in the spatial structure of a marine population can influence life  
49 history and demographic variations, which potentially affect its resilience to perturbations  
50 (Ciannelli et al. 2013).

51 What are the potential mechanisms shaping spatial segregation between body size  
52 groups of a population? Within a population, the distribution area of each body size group,  
53 and the distance between their abundance-weighted centers of distribution area (hereafter,  
54 centers of abundance), determine the overlapped area between them. On the one hand, when  
55 the distribution areas of two body size groups contract, their overlapped area declines,  
56 provided that their centers of abundance are fixed. On the other hand, elongated distance  
57 between the centers of abundance reduces the overlapped area between body size groups,  
58 provided that their areas of distribution are fixed.

59 Ocean warming and population decline potentially impact the area of distribution  
60 and the center of abundance of body size groups (Barnett et al. 2017, Orio et al. 2017).  
61 These impacts are likely size-specific. For example, earlier studies showed that ocean  
62 warming and fishing altered the abundance of body size groups at various extents (Barnett  
63 et al. 2017, Orio et al. 2017). Such size-specific changes in abundance could lead to  
64 differential changes in their area of distribution, based on abundance-distribution  
65 relationships and density-dependent habitat selection (MacCall 1990, Fisher and Frank 2004,  
66 Thorson et al. 2016). In addition, previous findings suggest that ocean warming and fishing  
67 contributed to size-specific shift in spatial distribution (Barbeaux and Hollowed 2018, Frank  
68 et al. 2018). This is due to thermal tolerance, food requirements, spatial constraints, and  
69 mobility that vary with body sizes within a population (Dahlke et al. 2020, Ciannelli et al.  
70 2022). Depending on the original positions of the center of abundance, the size-specific shift  
71 could increase the distance between their distribution. Linking body size-specific  
72 distribution response to ocean warming and population decline is key to understanding the

73 mechanisms behind the changes in spatial segregation between body size groups of a  
74 population.

75 In this study, we quantified and explored the mechanisms of changes in spatial  
76 segregation over time between body size groups within fish populations. We asked the  
77 following question: did the overlapped area of body size groups within populations decline  
78 over time, and what are the mechanisms behind? We studied fish populations in the North  
79 Sea, a global warming hotspot that has experienced rising sea surface temperature over the  
80 past decades (Hobday and Pecl 2014). Particularly, we focused on those fish populations  
81 that are ecologically and economically important and experienced large geographical re-  
82 distribution over the past century (Huserbråten et al. 2018), including Atlantic cod (*Gadus*  
83 *morhua*), haddock (*Melanogrammus aeglefinus*), and whiting (*Merlangius merlangius*).  
84 The total biomass of these populations has declined since 1980s with slow recovery in recent  
85 years (Engelhard et al. 2014). Therefore, these populations are prone to distribution area  
86 contraction and fragmentation. We analyzed their spatial dynamics using 43-year (1977-  
87 2019) winter survey data. We hypothesized that the body size groups of these populations  
88 became spatially more segregated over time, which was associated with contracted  
89 distribution area of body size groups, and/or elongated distance between centers of  
90 abundance of these groups. In addition, these changes were caused by body size-specific  
91 responses to environmental stress, including ocean warming and population decline.

## 92 **Materials and Methods**

### 93 Fish populations and survey data

94 The North Sea is a European epicontinental sea connected to the Atlantic Ocean.  
95 The north part of the North Sea is deeper, colder with higher salinity, while the south part  
96 is warmer, shallower with higher primary productivity. The North Sea has experienced

97 rising sea temperature and intensive fishing activities over the past decades (Murgier et al.  
98 2021). Fishing has been more intensive in the south part of the North Sea (Engelhard et al.  
99 2014).

100 We focused on three fish populations in the North Sea: Atlantic cod, haddock and  
101 whiting. They belong to the *Gadidae* family and are demersal populations which live just  
102 above the bottom of the sea (for life histories of three populations see **Table S1**). They have  
103 spawning migration in winter (Tobin et al. 2010, González-Irusta and Wright 2016).  
104 Evidence have shown that North Sea Atlantic cod is a metapopulation composed of three  
105 subpopulations: South, Northwest, and Viking (ICES 2020).

106 We obtained the survey data of three target populations from the online database of  
107 the International Bottom Trawl Survey (IBTS) of International Council for Exploitation of  
108 the Sea (ICES) (<https://data.ices.dk/>). This survey follows a stratified sampling on survey  
109 rectangles of  $1^\circ$  longitude  $\times$   $0.5^\circ$  latitude. The dataset is in the form of catch per unit effort  
110 (CPUE) per body size (in 10mm unit) for each rectangle and year-quarter. We extracted the  
111 winter data (January to February) between year 1977 and 2019 as our study period, because  
112 fishing gear was not standardized until 1977. We did not analyze the summer data, because  
113 the survey period is relatively short (starting from 1991), and that seasonal differences in  
114 the spatial structure is out of the scope of our study.

#### 116 Define body size groups within populations

117 We examined the spatial dynamics at the body size level. We followed the most  
118 common approach for body size grouping through dividing a population into equal body  
119 size bins (Barbeaux and Hollowed 2018, Li et al. 2019, Yang et al. 2019). We first summed  
120 the CPUE for each body size bin (in 1mm unit) over time and survey rectangle, to derive  
121 body size distribution. As the distribution was right-skewed, we removed individuals below

122 5% and above 85% quantile to avoid extremely low abundance at both ends. Then, we  
123 divided the body size distribution into equal-interval body size groups.

124 We tested different body size group number (10, 15, and 20 groups) to see how it  
125 influenced the value of spatial dynamics. While higher size group number gave higher  
126 precision, the spatial dynamics did not differ with group number (**Table S2**). We thus  
127 reported the results with 20 body size groups in the main text. We did not use group number  
128 higher than 20, otherwise would leads to too few individuals for largest and smallest body  
129 size groups; this could raise uncertainty of the results.

130 Deriving fixed number of body size group for each population leads to wider body  
131 size bins for larger populations, and narrower body size bins for smaller populations. To  
132 confirm the temporal dynamics of spatial overlap within populations, we alternatively  
133 derived body size groups by using fixed bin width for all three populations (e.g., 5 cm).

134 We also examined the changes in the overlapped area over time between life stages  
135 within populations as a preliminary test. To do so, we grouped each population into juvenile  
136 and adult, based on the body size at 50% maturity (**Table S1**).

137 We did not analyze the spatial structure using age groups because existing age-  
138 specific data did not distinguish age groups older than six years. Thus, spatial dynamics  
139 calculated using this dataset would neglect the dynamics between older groups. In addition,  
140 body size interval differed from one age to another due to non-linear age-size relationships.  
141 Because the results from age group or size group are not comparable, we reported only  
142 spatial structure between body size groups in this work.

#### 143 144 Spatial structure indices

145 To explore the temporal changes in the spatial distribution of body size groups  
146 within populations, we calculated the following indices for each survey year: 1) area of

147 distribution of each body size group, 2) center of abundance of each body size group, 3)  
 148 overlapped area between pairs of body size groups, and 4) distance between centers of  
 149 abundance of pairs of body size groups. There is a total of 190 ( $C_2^{20}$ ) pairs of body size  
 150 groups between 20 body size groups within a population.

151 The area of distribution of each body size group is the proportion of occupied area  
 152 at any given year, over the maximum occupied area of the same body size group over the  
 153 study period. This standardized measure accounts for variations in the occupied area  
 154 between different body size groups. Thus, this measure allows us to directly comparing  
 155 distribution area between different body size groups. The occupied area of a body size group  
 156 at a given year is defined as the number of survey rectangles where the CPUE of this group  
 157 is greater than zero. Therefore, the area of distribution of body size group  $i$  at year  $t$  is  
 158  $N_{i,t}/Max(N_i)$ , where  $N_{i,t}$  is the number of rectangles with the non-zero CPUE of body size  
 159 group  $i$  at year  $t$ , and  $Max(N_i)$  is the maximum number of rectangles of body size group  $i$   
 160 over the study period.

161 Center of abundance is CPUE-weighted center of occupied area for each body size  
 162 group. For body size group  $i$  at year  $t$ , the center of abundance in longitude is  $CEN_{i,t,lon}$   
 163  $= \sum_{r=1}^N CPUE_{i,r,t} \times lon_r / \sum_{r=1}^N CPUE_{i,r,t}$ , where  $lon_r$  is the longitudinal center of  
 164 rectangle  $r$ , and  $N$  is the number of survey rectangles where the CPUE of the whole  
 165 population is greater than zero. Similarly, the center of abundance in latitude  $CEN_{i,t,lat} =$   
 166  $\sum_{r=1}^N CPUE_{i,r} \times lat_r / \sum_{r=1}^N CPUE_{i,r}$ , where  $lat_r$  is the latitudinal center of rectangle  $r$ .

167 The overlapped area for a given pair of body size groups are indicated by union  
 168 overlapped area, and partial overlapped area. Union overlapped area is the proportion of co-  
 169 occupied area, over the area where either of the body size group occupies. For body size  
 170 group  $i$  and  $j$  at year  $t$ , the union overlapped area is  $N_{intersect,i,j,t}/N_{union,i,j,t}$ , where  
 171  $N_{intersect,i,j,t}$  is the number of rectangles where both body size group  $i$  and  $j$  have CPUE

greater than zero at year  $t$ , and  $N_{union,i,j,t}$  is the number of rectangles where either body size group  $i$  or  $j$  has CPUE greater than zero at year  $t$ . Partial overlapped area is proportion of co-occupied area over the occupied area of each body size group of the pair and then taken average. For body size group  $i$  and  $j$  at time  $t$ , partial overlapped area is  $0.5 \times (N_{intersect,i,j,t}/N_{i,t} + N_{intersect,i,j,t}/N_{j,t})$ . The concepts of distributional overlap has been used in inter-species co-occurrence at the community level (Griffith et al. 2018, Carroll et al. 2019), but not at the body size level.

The distance between centers of abundance is the longitudinal or latitudinal distance between centers of occupied area of a pair of body size groups. For body size group  $i$  and  $j$  at year  $t$ , the distance between centers of abundance in longitude is  $|CEN_{i,t,lon} - CEN_{j,t,lon}|$ , while the distance between centers of abundance in latitude is  $|CEN_{i,t,lat} - CEN_{j,t,lat}|$ .

Atlantic cod has three subpopulations in the North Sea (ICES 2020). Thus, we calculated the spatial structure of Atlantic cod at both the regional scale, as well as at the spatial scale concerning each subpopulation.

### Population biomass decline

We used the estimates of yearly total stock biomass from the ICES stock assessment (ICES 2016, 2018) as a proxy for population depletion level (Zhou et al. 2017). Total stock biomass showed a declining trend from 1977 to 2019 for all three populations (**Fig. S1**).

### Ocean warming

We used sea bottom temperature as an indicator of ocean warming, because all three target populations are demersal species. We obtained the sea bottom temperature of the CTD stations across the North Sea region from the ICES online database. We obtained the yearly winter sea bottom temperature at the North Sea region by averaging the

197 measurements from all CTD stations at each year. Sea bottom temperature in the North Sea  
198 exhibited a temporal increase from 1977 to 2019 (**Fig. S1**).

### 199 Statistical Analysis

200 The statistical models were constructed separately for each target population. We  
201 applied a four-step analysis are as follows:

202 (1) We used linear mixed-effects models to examine the temporal trends in the overlapped  
203 area of pairs of body size groups. Overlapped area of 190 paired groups was included  
204 as the response variable (not averaged but as 190 measures). Overlapped area is count-  
205 based percentage data. Therefore, it was logit-transformed before model fitting for better  
206 homoscedasticity. Survey year was normalized and fitted as a fixed effect. The id of  
207 paired groups nested within the survey year was fitted as a random effect. This allows  
208 for random intercept and slope for each pair of body size group. We repeated the same  
209 analysis to examine the temporal trends in the distance between centers of abundance  
210 for pairs of body size groups, without transforming the response variable. Then, we  
211 repeated the analysis to examine the temporal trends in the area of distribution of body  
212 size groups. Area of distribution is continuous proportional data. Thus, it was logit-  
213 transformed before fitting. The id of body size group nested within survey year was  
214 fitted as random effect.

215 (2) Then, we constructed a multiple regression model to test the relative importance of area  
216 of distribution and distance between centers of abundance on overlapped area. We  
217 regressed yearly mean of overlapped area (mean of 190 paired groups) against yearly  
218 mean of area of distribution (mean of 20 body size groups), and yearly mean of distance  
219 between centers of abundance in latitude and longitude (mean of 190 paired groups).  
220 This resulted in 43 data points (43 years) in each model. To account for serial correlation  
221 in time series data, we included the temporal autocorrelation of one-step time lag (AR1).

222 For the initial model, we included an interaction term between area of distribution and  
223 the distance between centers of abundance. As none of the interaction term was  
224 significant for neither population, we removed the interaction term from the initial  
225 model. The final model wrote:

226 Yearly mean of overlapped area across paired groups  $\sim \beta_1$  Yearly mean of area of  
227 distribution across body size groups +  $\beta_2$  Yearly mean of distance between centers  
228 of abundance in longitude across paired groups +  $\beta_3$  Yearly mean of distance  
229 between centers of abundance in latitude across paired groups + AR1,

230 where  $\beta$  represents the fixed effects coefficients. All explanatory variables were  
231 normalized before fitting. All the explanatory variables had variance inflation factors <  
232 6, suggesting no noticeable multicollinearity. We extracted the fixed effects coefficients  
233 with 95% confidence intervals to represent the relative importance of each explanatory  
234 variable.

235 (3) For each body size group, we evaluated the temporal trends in the area of distribution  
236 and center of abundance. To do so, we fitted a simple linear regression model for each  
237 body size group separately. We included the area of distribution (logit-transformed), or  
238 center of abundance of a body size group, as the response variable. We included survey  
239 year as the explanatory variable. We used the slope coefficient to indicate the rate of  
240 change in the area of distribution or center of abundance. Then, we examined how the  
241 rate of change varied with body size. To do so, we used nonparametric loess regression  
242 models. We included the rate of change in area of distribution, or center of abundance,  
243 as the response variable. We included body size group as a continuous explanatory  
244 variable.

245 (4) Finally, we examined whether the overlapped area was influenced by sea bottom  
246 temperature (Temperature) and total stock biomass (Biomass). In addition, we examined

247 how the effects differed between body size groups within each fish population. We  
248 hypothesized that the overlapped area is shaped by the area of distribution, and center  
249 of abundance of each body size group. Therefore, we examined the effects of  
250 Temperature and Biomass on these two variables. Temperature and Biomass are highly  
251 colinear for three populations. Thus, we tested their effects using separate models. In  
252 addition, we included AR1 in the model to account for the temporal autocorrelation. The  
253 four full models were:

- 254 i. Yearly area of distribution of each body size group  $\sim \beta_1$  body size group id  $\times$   
255 yearly Temperature +  $\beta_2$  CPUE + AR1, and
- 256 ii. Yearly area of distribution of each body size group  $\sim \beta_1$  body size group id  $\times$   
257 Biomass +  $\beta_2$  CPUE + AR1, and
- 258 iii. Yearly center of abundance of each body size group in longitude or latitude  $\sim \beta_1$   
259 body size group id  $\times$  Yearly Temperature + AR1, and
- 260 iv. Yearly center of abundance of each body size group in longitude or latitude  $\sim \beta_1$   
261 body size group id  $\times$  Yearly Biomass + AR1,

262 where log-transformed CPUE of each body size group was included as a covariate to  
263 account for abundance-distribution relationships. From each full model, we performed  
264 a backward stepwise model selection. We derived the most parsimonious model based  
265 on AIC and  $R^2$  values.

266 We performed linear mixed-effects models using the function *lmer* from the *lme4* package.  
267 *P-values* were extracted using *lmerTest* package. We extracted Conditional  $R^2$  (variance  
268 explained by both fixed and random effects) from the function *r.squaredGLMM* of *MuMIn*  
269 package. We performed the loess regression model with the *geom\_smooth* function of  
270 *ggplot2* package. We further used heatmaps to visualize the differences in the temporal  
271 trends of overlapped area between each pair of size groups.

## 272 **Results and Discussion**

### 273 Temporal decline in overlapped area between body size groups

274 For all three populations between 1977 and 2019, the overlapped area between pairs  
275 of body size groups declined; that is, the spatial segregation increased between 20 body size  
276 groups (**Fig. 1**). The declining trends were significant regardless of the number of size  
277 groups we defined for each population (from 10 to 20 size groups, see **Table S2**), or fixed  
278 size bin width (e.g., 5cm, **Fig S2**). In addition, the declining patterns were observed for each  
279 subpopulation of Atlantic cod (South, Northwest, and Viking) (**Table S3**), suggesting a  
280 universal declining spatial overlap for the Atlantic cod metapopulation.

281 For Atlantic cod, the decline in spatial overlap was strong between small groups,  
282 between large groups, and between small and large groups (**Fig. S3**). Supporting these  
283 results, we observed clear declines over time in the number of co-occupied survey rectangles  
284 between juvenile and adult stages (**Fig. S4**). In contrast, for haddock, the decline in spatial  
285 overlap occurred only between small size groups (**Fig. S3**). Similarly, whiting showed  
286 declining spatial overlap between smaller groups, but increasing spatial overlap between  
287 larger groups (**Fig. S3**). The lack of changes in the spatial overlap between small and large  
288 groups, for both haddock and whiting, explained why the changes in co-occupied survey  
289 rectangles between juvenile and adult stages are less drastic compared to Atlantic cod (**Fig.**  
290 **S5 – S6**).

### 292 Contraction of the area of distribution of body size groups

293 One mechanism of spatial segregation between body size groups over time was  
294 related to the contraction of their distribution area, driven by rising sea temperature and/or  
295 population biomass decline. This mechanism was strongest in Atlantic cod and haddock.

296 The mechanism was weaker in whiting, which exhibited contraction of distribution area for  
297 smaller groups but expansion for larger groups over time.

298 Particularly, for Atlantic cod and haddock, the mean distribution area across body  
299 size groups declined over time (**Fig. 2a-b**). The mean distribution area was positively  
300 associated with the mean overlapped area across pairs of body size groups (**Fig. 3a-b**). In  
301 addition, total stock biomass positively contributed to the distribution area of each body size  
302 group (**Fig. 4a-b**). These results suggest that declining total stock biomass over time for  
303 these two populations (**Fig. S1**) led to contracted distribution area of body size groups,  
304 which in turn decreased their overlapped area. Particularly, during the latter years with  
305 lower stock biomass, larger size groups of Atlantic cod contracted their distribution areas in  
306 a greater rate than smaller groups ( $P < 0.0001$  for an interactive term of total stock biomass  
307  $\times$  body size group, **Fig. 4a, Table S4**). This pattern implies a greater removal of larger  
308 groups under intensive fishing exploitation time period (Horwood et al. 2006, Hsieh et al.  
309 2010a). The positive association between population biomass and the area of distribution of  
310 body size groups agrees with the positive relationship observed at the whole population  
311 level of many fish species, as a result of density-dependent habitat selection (Fretwell and  
312 Lucas 1970, MacCall 1990, Fisher and Frank 2004, Thorson et al. 2016). Our finding is also  
313 supported by earlier evidence that during low abundance years, the area of distribution of  
314 age-1 and age-2 North Sea cod contracted to less than half of that available, towards habitats  
315 that have near-optimal bottom temperatures (Blanchard et al. 2005).

316 Overfishing is a potential main reason for biomass decline and spatial segregation  
317 within the Atlantic cod population. However, we did not examine the direct impact of  
318 fishing activity (i.e., fishing mortality) on spatial dynamics of Atlantic cod. It is because  
319 Atlantic cod is categorized as overexploited species, and its biomass recovers very slowly  
320 even after relaxing the fishing pressure since 1990s (Köster et al. 2014). Thus, instantaneous

321 fishing mortality measured at each year does not reflect the long-term impacts of fishing on  
322 the biomass and spatial structure of the population. Thus, in this study, we used estimated  
323 total stock biomass as the indicator of population depletion level (Froese et al. 2017) rather  
324 than fishing mortality, as a proxy to examine long-term fishing impacts on population spatial  
325 dynamics.

326 In contrast to Atlantic cod and haddock, whiting did not have a significant decline  
327 in the mean distribution area across body size groups (**Fig. 2c**). It was because larger groups  
328 expanded their distribution area while smaller groups contracted their distribution area over  
329 time (**Fig. 4c**). However, the mean area of distribution across body size groups was still  
330 positively related to their overlapped area (**Fig. 3c**).

331 In addition to the effect of population biomass decline, ocean warming also impacted  
332 the distribution area of body size groups, and the impacts varied among populations. For  
333 haddock, sea bottom temperature negatively explained the area of distribution of all body  
334 size groups (slope coefficient  $\pm$  standard error =  $-0.012 \pm 0.004$ ,  $P < 0.005$ , **Fig. 4b**, **Table**  
335 **S4**). That is, the rising temperature over the study period contributed to the contraction of  
336 the distribution area of all body size groups, which then reduced the overlapped area  
337 between them (**Fig. 3b**). In contrast, for whiting, rising sea temperature resulted in the  
338 contraction of the distribution area of smaller size groups, but expansion of distribution area  
339 of large sizes groups ( $P < 0.01$  for the interactive term of sea bottom temperature  $\times$  body  
340 size group, **Fig. 4c**). The differential responses between smaller and larger groups explains  
341 the lack of temporal patterns in the mean area of distribution across body size groups of  
342 whiting (**Fig. 2c**). In contrast to haddock and whiting, the distribution area of body size  
343 groups of Atlantic cod was determined by the population biomass but not by the sea bottom  
344 temperature (**Fig 4a**).

345 We speculate that the differences between haddock and whiting, in their distribution  
346 area response to ocean warming, may be due to their prey types. Haddock, regardless of  
347 body size, mainly feeds on benthic organisms which are spatially restricted under  
348 environmental changes (Schückel et al. 2010). In contrast, whiting is one of the top marine  
349 predators feeding on fishes, such as Norway pout, sandeel and sprat (Hislop et al. 1991).  
350 These fish prey have higher dispersal potential than benthic organisms under environmental  
351 changes, and thus could lead to the expansion of distribution for adult whiting that followed  
352 their prey. This is supported by otolith microchemistry analysis, showing that adult whiting  
353 can travel long distances (>500 km) to faraway spawning areas (Tobin et al. 2010). Whereas,  
354 contrary to larger size whiting, the distribution area of small size whiting contracted over  
355 time (**Fig 4c**). These observations support the notion that larger groups of some fish  
356 populations can be resistant to adverse conditions related to warming, and could have better  
357 knowledge and higher mobility moving to the optimal foraging and spawning grounds  
358 (Hsieh et al. 2010a).

359 Haddock and whiting have shifted northward since 1977, and the shift of whiting  
360 was correlated with warming (Perry et al. 2005). If some fishes have shifted outside of the  
361 North Sea, then the population biomass within the North Sea may reduce, leading to  
362 contraction in the distribution area and then spatial segregation between body size groups.  
363 Nevertheless, the spatial overlap indices used in our study is not sensitive to the spatial  
364 boundary of populations. This is because the indices are calculated based on the ratio of co-  
365 occupied area over occupied area by each body size group. Thus, these indices reveal the  
366 temporal variations in the degree of spatial overlap within the region analyzed in this study.

367  
368 Distance increased between the centers of abundance between body size groups

369 In addition to the area of distribution, we hypothesized that the overlapped area  
370 between body size groups were negatively associated with their distance between the centers  
371 of abundance. In addition, such pattern was due to body size-specific shift in the centers of  
372 abundance, responding to rising sea temperature or population biomass decline. We found  
373 that whiting was the only population that exhibited this mechanism. In contrast, the spatial  
374 overlap within Atlantic cod and haddock was mainly determined by the area of distribution  
375 of body size groups.

376 Particularly, whiting showed temporal increases in the mean distance between  
377 centers of abundance across pairs of body size groups in longitude and latitude (**Fig. 2 f, i**).  
378 In addition, the mean distance was negatively associated with the overlapped area across  
379 paired groups (**Fig. 3c**). These results suggest that an increase in the distance contributed to  
380 a decline in the overlap between body size groups. The center of abundance of larger whiting  
381 shifted westward, while smaller groups shifted eastward ( $P < 0.005$  for an interactive term  
382 of sea bottom temperature  $\times$  body size group id, **Table S4, Fig. 4f**). Therefore, depending  
383 on the original position of distributions, the body size-varying shift in the centers of  
384 abundance may have increased the distance between body size groups, hence reducing their  
385 overlapped area.

386 In contrast to whiting, for Atlantic cod and haddock, the distance between the centers  
387 of abundance across paired groups did not significantly explain the overlapped area (**Fig.**  
388 **3a-b**). However, both populations showed an increase in the distance between centers of  
389 abundance (except for Atlantic cod at the longitudinal distance) (**Fig 2d-e, 2g-h**). These  
390 results suggest that the changes in the distance were too weak to influence the overlapped  
391 area between body size groups. Instead, the contraction of area of distribution of body size  
392 groups was the main driver for the spatial segregation under lower population biomass for  
393 Atlantic cod and haddock (**Fig 3a-b**). Interestingly, for haddock, the center of abundance of

394 larger groups at latitudinal direction was more negatively associated with the sea bottom  
395 temperature, compared to smaller haddock ( $P < 0.01$  for an interactive term of sea bottom  
396 temperature  $\times$  body size group id, **Fig. 4h, Table S4**). Consequently, the centers of  
397 abundance of all size groups shifted northward in response to higher temperature, but larger  
398 size groups shifted faster than smaller size groups. Such different magnitudes of shift of the  
399 centers of abundance of body size groups in response to warming may have led to increased  
400 distance between their distributions for haddock.

## 402 Implications

403 While all the populations examined in this study demonstrated increased spatial  
404 segregation between body size groups over time, the underlying spatial dynamics of body  
405 size groups (i.e., area of distribution and center of abundance) and driving forces (i.e., ocean  
406 warming and population biomass decline) differed among the three studied populations (**Fig.**  
407 **5**). These results have important implications for exploring the differences between  
408 populations in their physiological and biogeographic traits at the body size level. For  
409 example, body size groups within a population can exhibit different niches (e.g., thermal  
410 tolerance, food requirements (Ciannelli et al. 2013)). What drives different spatial responses  
411 among populations depends on the extent to which the niches of body size groups overlap.  
412 For example, populations with stronger or weaker niche preferences between body size  
413 groups may respond differently to disturbances such as climatic or anthropogenic stress  
414 (Tao et al. 2021).

415 For Atlantic cod and haddock, the contraction of the distribution area of body size  
416 groups was the main driver for the spatial segregation among body size groups over time.  
417 This finding has important implications to identify populations at risk of increased spatial  
418 segregation at body size group level. For example, both highly migratory pelagic predators  
419 (e.g., tuna, billfish) (Worm and Tittensor 2011) and species living in regional seas (e.g.,

420 Monterey Spanish mackerel at the coast of California (Collette and Russo 1984) and  
421 yellowtail flounder around Newfoundland (Brodie et al. 1998)) have shown contraction of  
422 their distribution area over the past decades. Although the contractions of distribution area  
423 were observed at the population level, these patterns may apply to the finer level of body  
424 size group. Furthermore, global projections estimated that the biomass of 77% of exploited  
425 fishes and invertebrates will decrease when high-temperature extreme will occur (Cheung  
426 et al. 2021). These pieces of evidence imply that many fish populations may have exhibited  
427 spatial segregation between body size groups, especially for those underwent reduced  
428 population biomass and contracted area of distribution, and for those living in climate-  
429 unstable regions. Large distributional shift may also reduce population biomass and  
430 distributional area at the original habitats. For example, in the North Sea, nearly two-third  
431 of fish species have shifted northward or deeper between 1977 and 2001 (Perry et al. 2005).  
432 Further investigations on these species which are “on the move” in the North Sea and  
433 beyond can help identify the state of the art of spatial dynamics within these populations,  
434 and to examine the spatial mechanisms and drivers for these vulnerable populations. These  
435 results are helpful to prioritize management and conservation efforts.

436 The ecological consequences of spatial segregation between body size groups of a  
437 population needs further investigation. While population growth may increase due to  
438 weakened cannibalism and competition, spatial segregation of size groups may increase the  
439 vulnerability of demographic structure to local perturbations. This merits future research to  
440 investigate the net effects of within-population spatial segregation on population dynamics  
441 and stability.

## 442 **Conclusion**

443 Recently, increasing evidence on aquatic and terrestrial populations has shown that  
444 the shift in spatial distribution varied between life stages or body size under environmental  
445 change (Bell et al. 2015, Máliš et al. 2016, Fei et al. 2017, Barbeaux and Hollowed 2018,  
446 Frank et al. 2018, Yang et al. 2019). However, it remains unclear to what extent different  
447 size groups within populations has segregated from each other over time. We develop a new  
448 analytical approach to deepen the understanding of spatial dynamics within populations  
449 under global environmental stress. This approach can be applied to populations at various  
450 terrestrial and aquatic ecosystems globally, to identify vulnerable populations under  
451 environmental stress. This approach also allows us to uncover the mechanisms of spatial  
452 segregation within populations, which have profound consequences in demographic  
453 connectivity and population stability.

#### 454 **Data and availability statements:**

455 All raw data that support the findings of this study are publicly available. Fish survey data  
456 and sea bottom temperature are available at the ICES data portal <https://data.ices.dk/>. Total  
457 stock biomass is available from ICES stock assessment reports (ICES 2016, 2018). The  
458 codes needed to replicate the analyses presented in this paper will be available at online  
459 repository.

#### 460 **References**

- 461 Barbeaux, S. J., and A. B. Hollowed. 2018. Ontogeny matters: Climate variability and effects on  
462 fish distribution in the eastern Bering Sea. *Fisheries Oceanography* 27:1–15.
- 463 Barnett, L. A. K., T. A. Branch, R. A. Ranasinghe, and T. E. Essington. 2017. Old-Growth Fishes  
464 Become Scarce under Fishing. *Current Biology* 27:2843-2848.e2.

465 Bell, R. J., D. E. Richardson, J. A. Hare, P. D. Lynch, and P. S. Fratantoni. 2015. Disentangling  
466 the effects of climate, abundance, and size on the distribution of marine fish: An example  
467 based on four stocks from the Northeast US shelf. *ICES Journal of Marine Science*  
468 72:1311–1322.

469 Blanchard, J. L., C. Mills, S. Jennings, C. J. Fox, B. D. Rackham, P. D. Eastwood, and C. M.  
470 O'Brien. 2005. Distribution-abundance relationships for North Sea Atlantic cod (*Gadus*  
471 *morhua*): observation versus theory. *Canadian Journal of Fisheries and Aquatic Sciences*  
472 62:2001–2009.

473 Brodie, W. B., S. J. Walsh, and D. B. Atkinson. 1998. The effect of stock abundance on range  
474 contraction of yellowtail flounder (*Pleuronectes ferruginea*) on the Grand Bank of  
475 Newfoundland in the Northwest Atlantic from 1975 to 1995. *Journal of Sea Research*  
476 39:139–152.

477 Carroll, G., K. K. Holsman, S. Brodie, J. T. Thorson, E. L. Hazen, S. J. Bograd, M. A. Haltuch, S.  
478 Kotwicki, J. Samhouri, P. Spencer, E. Willis-Norton, and R. L. Selden. 2019. A review of  
479 methods for quantifying spatial predator–prey overlap. *Global Ecology and Biogeography*  
480 28:1561–1577.

481 Cheung, W. W. L., T. L. Frölicher, V. W. Y. Lam, M. A. Oyinlola, G. Reygondeau, U. Rashid  
482 Sumaila, T. C. Tai, L. C. L. Teh, and C. C. C. Wabnitz. 2021. Marine high temperature  
483 extremes amplify the impacts of climate change on fish and fisheries. *Science Advances* 7.

484 Ciannelli, L., J. A. D. Fisher, M. Skern-Mauritzen, M. E. Hunsicker, M. Hidalgo, K. T. Frank, and  
485 K. M. Bailey. 2013. Theory, consequences and evidence of eroding population spatial  
486 structure in harvested marine fishes: A review. *Marine Ecology Progress Series* 480:227–  
487 243.

488 Ciannelli, L., A. B. Neuheimer, L. C. Stige, K. T. Frank, J. M. Durant, M. Hunsicker, L. A.  
489 Rogers, S. Porter, G. Ottersen, and N. A. Yaragina. 2022. Ontogenetic spatial constraints  
490 of sub-arctic marine fish species. *Fish and Fisheries* 23:342–357.

491 Collette, B. B., and J. L. Russo. 1984. Morphology, systematics, and biology of the Spanish  
492 mackerels ( *Scomberomorus*, Scombridae). *Fishery Bulletin* 82:545–692.

493 Dahlke, F. T., S. Wohlrab, M. Butzin, and H. O. Pörtner. 2020. Thermal bottlenecks in the life  
494 cycle define climate vulnerability of fish. *Science* 369:65–70.

495 Engelhard, G. H., D. A. Righton, and J. K. Pinnegar. 2014. Climate change and fishing: A century  
496 of shifting distribution in North Sea cod. *Global Change Biology* 20:2473–2483.

497 Fei, S., J. M. Desprez, K. M. Potter, I. Jo, J. A. Knott, and C. M. Oswalt. 2017. Divergence of  
498 species responses to climate change. *Science Advances* 3.

499 Fisher, J. A. D., and K. T. Frank. 2004. Abundance–distribution relationships and conservation of  
500 exploited marine fishes. *Marine Ecology Progress Series* 279:201–213.

501 Frank, K. T., B. Petrie, W. C. Leggett, and D. G. Boyce. 2018. Exploitation drives an ontogenetic-  
502 like deepening in marine fish. *Proceedings of the National Academy of Sciences of the*  
503 *United States of America* 115:6422–6427.

504 Fretwell, S. D., and H. L. Jr. Lucas. 1970. On territorial behavior and other factors influencing  
505 habitat distribution in birds. I. Theoretical development. *Acta Biotheor.* 19:16–36.

506 Froese, R., N. Demirel, G. Coro, K. M. Kleisner, and H. Winker. 2017. Estimating fisheries  
507 reference points from catch and resilience. *Fish and Fisheries* 18:506–526.

508 González-Irusta, J. M., and P. J. Wright. 2016. Spawning grounds of Atlantic cod ( *Gadus*  
509 *morhua* ) in the North Sea. *ICES Journal of Marine Science: Journal du Conseil* 73:304–  
510 315.

511 Griffith, G. P., P. G. Strutton, and J. M. Semmens. 2018. Climate change alters stability and  
512 species potential interactions in a large marine ecosystem. *Global Change Biology*  
513 24:e90–e100.

514 Hislop, J. R. G., A. P. Robb, M. A. Bell, and D. W. Armstrong. 1991. The diet and food  
515 consumption of whiting (*Merlangius merlangus*) in the north sea. *ICES Journal of Marine*  
516 *Science* 48:139–156.

517 Hobday, A. J., and G. T. Pecl. 2014. Identification of global marine hotspots: Sentinels for change  
518 and vanguards for adaptation action. *Reviews in Fish Biology and Fisheries* 24:415–425.

519 Horwood, J., C. O’Brien, and C. Darby. 2006. North Sea cod recovery? *ICES Journal of Marine*  
520 *Science* 63:961–968.

521 Hsieh, C. hao, A. Yamauchi, T. Nakazawa, and W. F. Wang. 2010a. Fishing effects on age and  
522 spatial structures undermine population stability of fishes. *Aquatic Sciences* 72:165–178.

523 Hsieh, C., A. Yamauchi, T. Nakazawa, and W. F. Wang. 2010b. Fishing effects on age and spatial  
524 structures undermine population stability of fishes. *Aquatic Sciences* 72:165–178.

525 Hughes, N. F., and T. C. Grand. 2000. Physiological ecology meets the ideal-free distribution:  
526 Predicting the distribution of size-structured fish populations across temperature gradients.  
527 *Environmental Biology of Fishes* 59:285–298.

528 Huserbråten, M. B. O., E. Moland, and J. Albretsen. 2018. Cod at drift in the North Sea. *Progress*  
529 *in Oceanography* 167:116–124.

530 ICES. 2016. Report of the Inter-Benchmark Protocol for Whiting in the North Sea (IBP Whiting).

531 ICES. 2018. Report of the Working Group on Assessment of Demersal Stocks in the North Sea  
532 and Skagerrak. Page ICES CM.

533 ICES. 2020. Workshop on Stock Identification of North Sea Cod.

534 Köster, F. W., R. L. Stephenson, and E. A. Trippel. 2014. Gadoid fisheries: The ecology and  
535 management of rebuilding. *ICES Journal of Marine Science* 71:1311–1316.

536 Li, L., A. B. Hollowed, E. D. Cokelet, S. J. Barbeaux, N. A. Bond, A. A. Keller, J. R. King, M.  
537 M. McClure, W. A. Palsson, P. J. Stabeno, and Q. Yang. 2019. Subregional differences in  
538 groundfish distributional responses to anomalous ocean bottom temperatures in the  
539 northeast Pacific. *Global Change Biology* 25:2560–2575.

540 Li, L., A. B. Hollowed, E. D. Cokelet, M. M. McClure, A. A. Keller, S. J. Barbeaux, and W. A.  
541 Palsson. 2022. Three-dimensional ontogenetic shifts of groundfish in the Northeast  
542 Pacific. *Fish and Fisheries* 23:1221–1239.

543 MacCall, A. D. 1990. Dynamic geography of marine fish populations. Washington Sea Grant  
544 Program, Seattle, Wash.

545 Máliš, F., M. Kopecký, P. Petřík, J. Vladovič, J. Merganič, and T. Vida. 2016. Life stage, not  
546 climate change, explains observed tree range shifts. *Global Change Biology* 22:1904–  
547 1914.

548 Marandel, F., P. Lorance, M. Andrello, G. Charrier, S. Le Cam, S. Lehuta, and V. M. Trenkel.  
549 2018. Insights from genetic and demographic connectivity for the management of rays and  
550 skates. *Canadian Journal of Fisheries and Aquatic Sciences* 75:1291–1302.

551 Murgier, J., M. Mclean, A. Maire, D. Mouillot, N. Loiseau, F. Munoz, C. Violle, and A. Auber.  
552 2021. Rebound in functional distinctiveness following warming and reduced fishing in the  
553 North Sea.

554 Orio, A., A. B. Florin, U. Bergström, I. Šics, T. Baranova, and M. Casini. 2017. Modelling  
555 indices of abundance and size-based indicators of cod and flounder stocks in the Baltic  
556 Sea using newly standardized trawl survey data. *ICES Journal of Marine Science*  
557 74:1322–1333.

558 Perry, A. L., P. J. Low, J. R. Ellis, and J. D. Reynolds. 2005. Climate change and distribution  
559 shifts in marine fishes. *Science* 308:1912–1915.

560 Schückel, S., S. Ehrich, I. Kröncke, and H. Reiss. 2010. Linking prey composition of haddock  
561 *Melanogrammus aeglefinus* to benthic prey availability in three different areas of the  
562 northern North Sea. *Journal of Fish Biology* 77:98–118.

563 Sunday, J. M., G. T. Pecl, S. Frusher, A. J. Hobday, N. Hill, N. J. Holbrook, G. J. Edgar, R.  
564 Stuart-Smith, N. Barrett, T. Wernberg, R. A. Watson, D. A. Smale, E. A. Fulton, D.  
565 Slawinski, M. Feng, B. T. Radford, P. A. Thompson, and A. E. Bates. 2015. Species traits  
566 and climate velocity explain geographic range shifts in an ocean-warming hotspot.  
567 *Ecology Letters* 18:944–953.

568 Tao, H. H., G. Dur, P. J. Ke, S. Souissi, and C. hao Hsieh. 2021. Age-specific habitat preference,  
569 carrying capacity, and landscape structure determine the response of population spatial  
570 variability to fishing-driven age truncation. *Ecology and Evolution* 11:6358–6370.

571 Thorson, J. T., A. Rindorf, J. Gao, D. H. Hanselman, and H. Winker. 2016. Density-dependent  
572 changes in effective area occupied for sea-bottom-associated marine fishes. *Proceedings*  
573 *of the Royal Society B: Biological Sciences* 283:20161853.

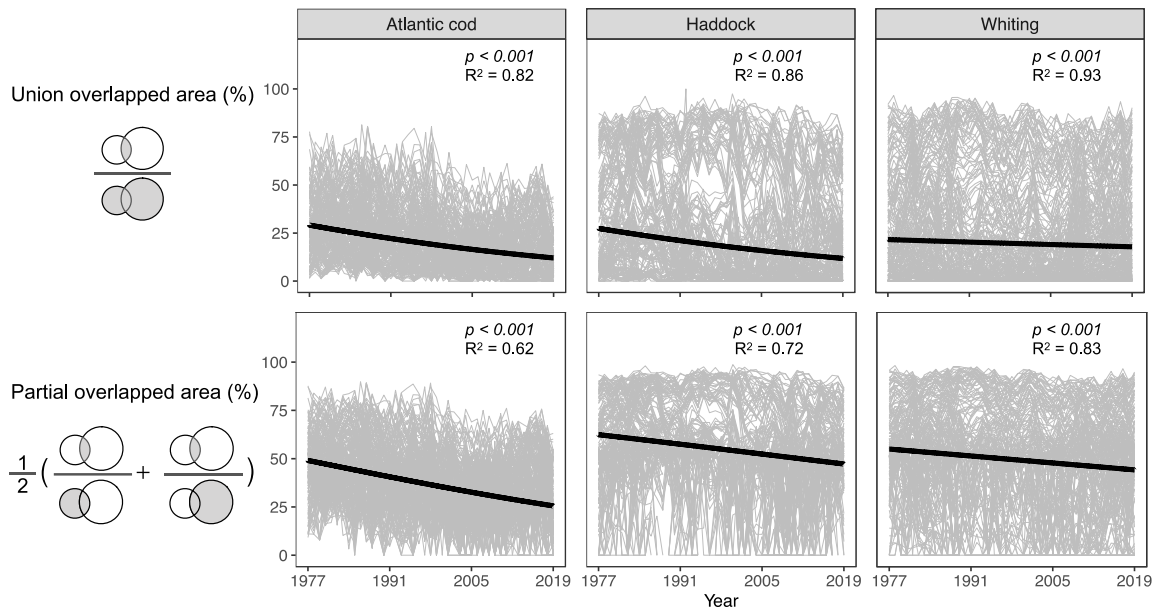
574 Tobin, D., P. J. Wright, F. M. Gibb, and I. M. Gibb. 2010. The importance of life stage to  
575 population connectivity in whiting (*Merlangius merlangus*) from the northern European  
576 shelf. *Marine Biology* 157:1063–1073.

577 Worm, B., and D. P. Tittensor. 2011. Range contraction in large pelagic predators. *Proceedings of*  
578 *the National Academy of Sciences of the United States of America* 108:11942–11947.

579 Yang, Q., E. D. Cokelet, P. J. Stabeno, L. Li, A. B. Hollowed, W. A. Palsson, N. A. Bond, and S.  
580 J. Barbeaux. 2019. How “The Blob” affected groundfish distributions in the Gulf of  
581 Alaska. *Fisheries Oceanography* 28:434–453.

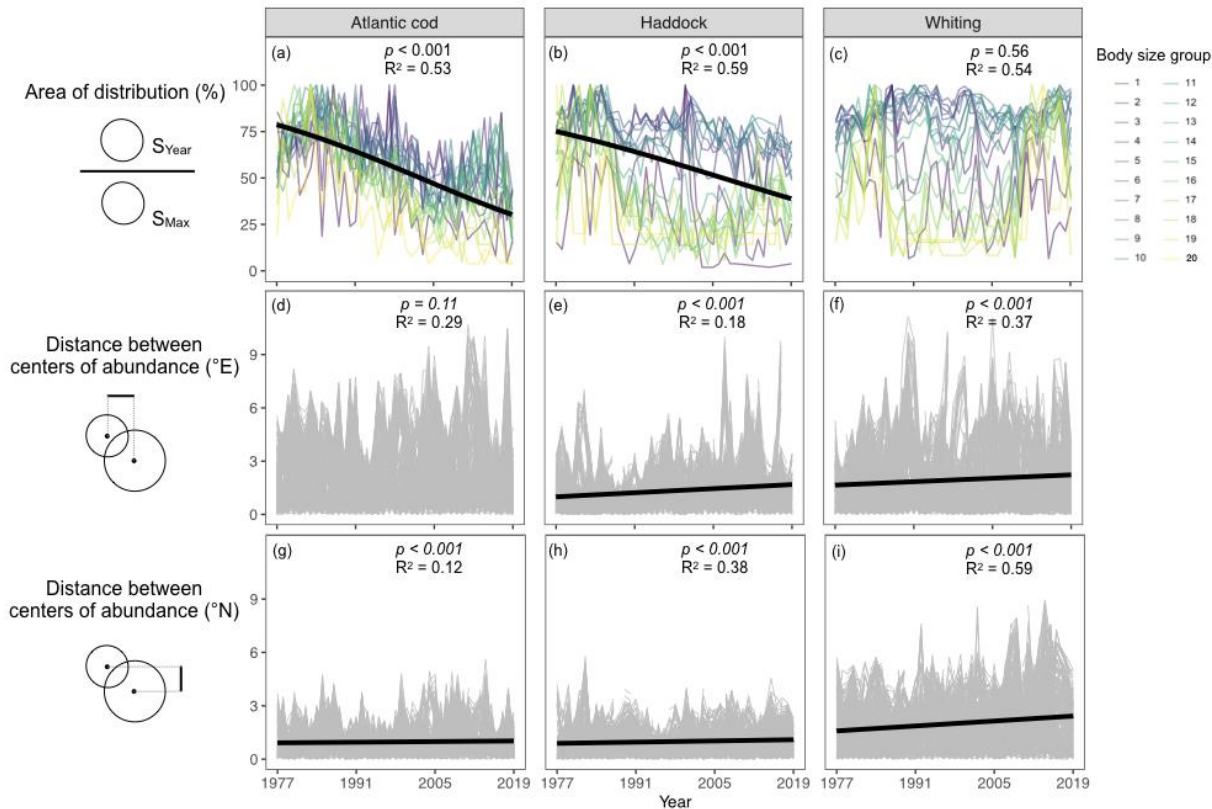
582 Zhou, S., A. E. Punt, Y. Ye, N. Ellis, C. M. Dichmont, M. Haddon, D. C. Smith, and A. D. M.  
583 Smith. 2017. Estimating stock depletion level from patterns of catch history. *Fish and*  
584 *Fisheries* 18:742–751.

585



587

588 **Fig. 1 Decline in the overlapped area between pairs of body size groups of three fish**  
 589 **populations between 1977 and 2019.** Each population is divided into 20 body size groups,  
 590 resulting in a total of 190 pairs of body size groups. Overlapped area was calculated as the  
 591 proportion of co-occupied area over the area where either body size group occupies (union  
 592 overlapped area, upper panel), and as the proportion of co-occupied area over the averaged area of  
 593 distribution of each body size group of the pair (partial overlapped area, lower panel). Yearly  
 594 overlapped area for each of the 190 body size group pairs is shown in grey thin line. The temporal  
 595 trend of overlapped area was examined using linear mixed-effects model, with logit-transformed  
 596 overlapped area as the response variable, survey year as the fixed effect, and pairs of body size  
 597 groups within year as the random effect. Black thick lines indicate the regression lines with slope  
 598 coefficients that were significantly different from zero according to F-test. Conditional  $R^2$  (which  
 599 considers variances of both fixed and random effects) were reported on the graphs. Marginal  $R^2$   
 600 (which considers only variances of fixed effects) for Atlantic cod, haddock, and whiting were 0.11,  
 601 0.03, 0.002 (union overlapped area) and 0.11, 0.04, and 0.006 (partial overlapped area), respectively.



602

603 **Fig. 2 Area of distribution (a-c) and distance between centers of abundance in longitude (d-f)**

604 **and latitude (g-i) between 1977 and 2019.** (a-c) Area of distribution of each body size group for

605 each year is calculated as the proportion of occupied area ( $S_{Year}$ ) over the maximum occupied area

606 over the study period ( $S_{Max}$ ). Colored lines indicate time series of 20 body size groups. We

607 performed linear mixed-effects models, with logit-transformed area of distribution as the response

608 variable, year as the explanatory variable, and body size group nested within year as the random

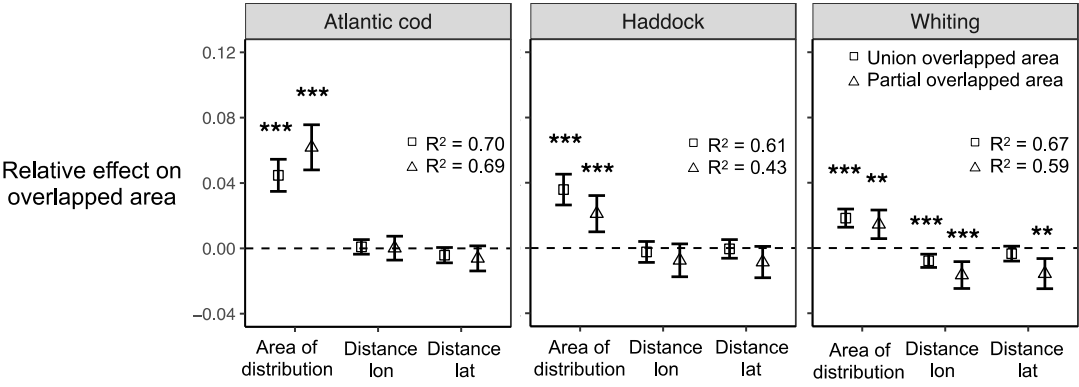
609 effect. (d-i) Each grey line indicates the time series of one of 190 pairs of body size groups. We

610 performed linear mixed-effects models, with the distance between centers of distribution as the

611 fixed effect, survey year as the fixed effect, and pairs of body size groups nested within year as the

612 random effect. Black thick lines indicate significant models ( $p < 0.05$ ), while nonsignificant results

613 are now shown.



615

616 **Fig. 3 Effects of area of distribution and distance between centers of abundance on overlapped**

617 **area.** Relative effects were derived from slope coefficients of multiple linear regression models,

618 including overlapped area as the response variable, area of distribution of each body size group and

619 distance between centers of abundance of pairs of body size groups (in longitude and latitude) as

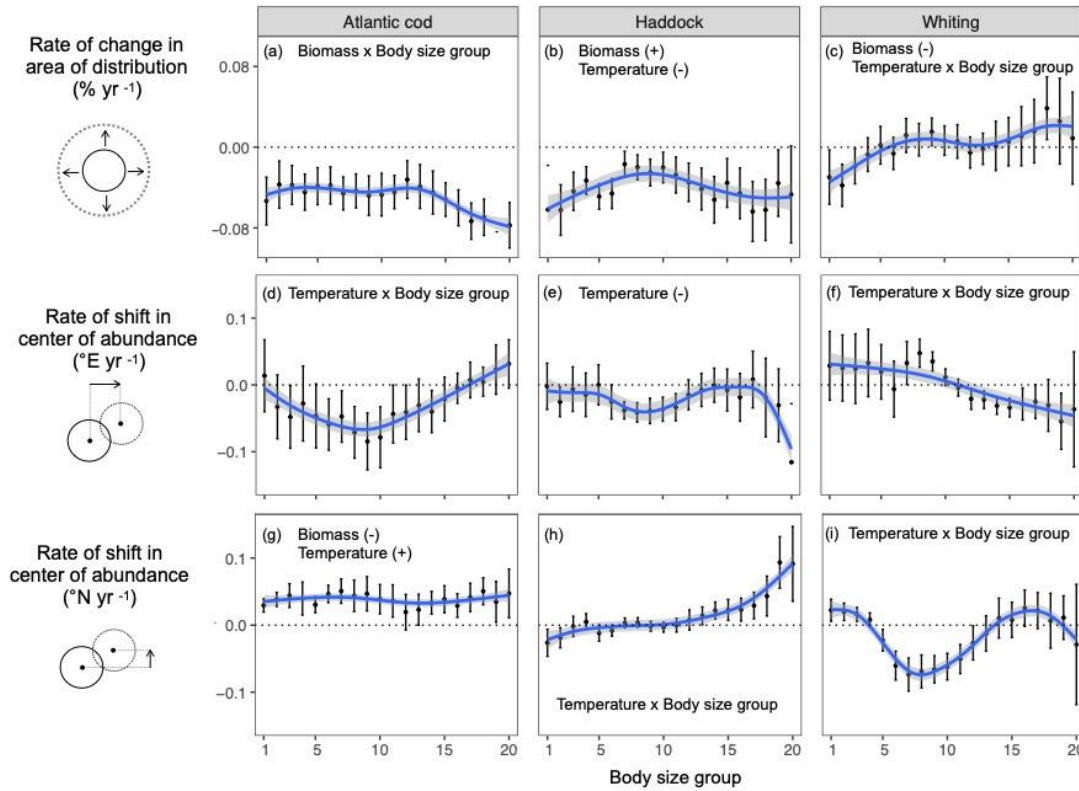
620 explanatory variables, and an AR1 term. Response and explanatory variables were yearly mean

621 values across all body size groups (for area of distribution) or across all pairs of body size groups

622 (for overlapped area and distance between centers of abundance). Bars indicate 95% confidence

623 intervals. Dotted horizontal line indicates zero slope coefficient. \*\*\*  $p < 0.001$ , \*\*  $p < 0.01$ , and \*

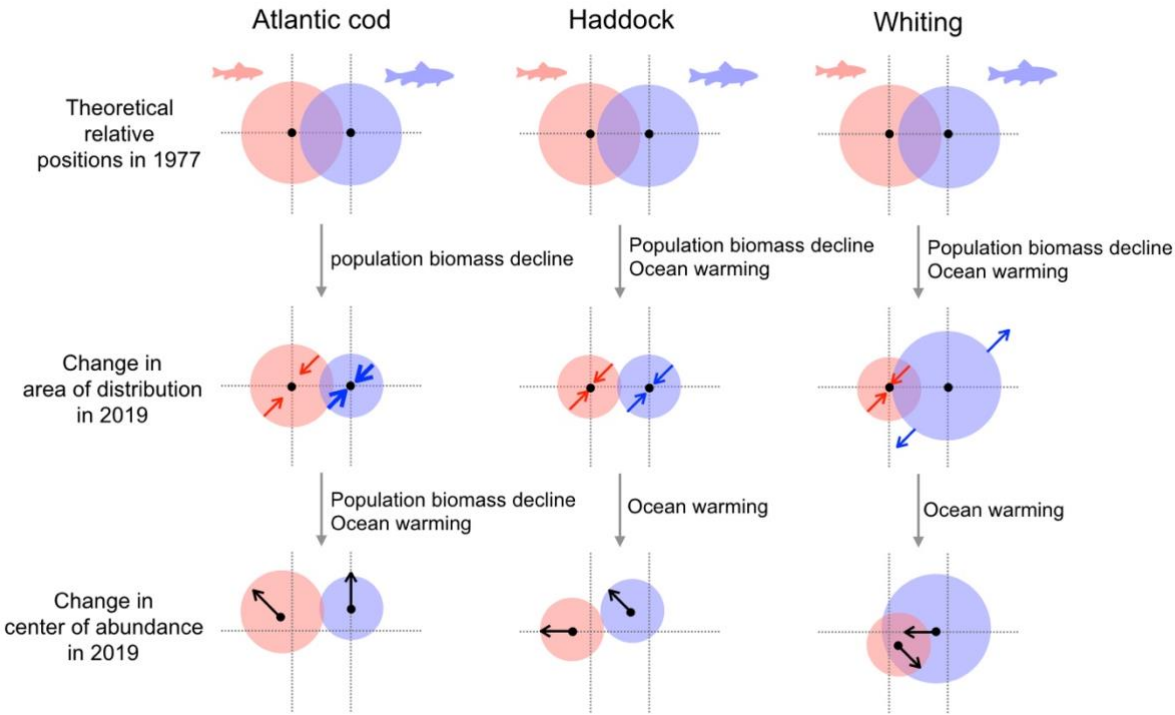
624  $p < 0.05$  indicate that the slope coefficient is significantly different from zero according to F-test.



626

627 **Fig. 4 Rate of change in the area of distribution and center of abundance between 1977 and**  
 628 **2019 in response to ocean warming and population biomass decline.** The rate of change for each  
 629 body size group was indicated by the temporal slope (point) of linear regression model, including  
 630 area of distribution or center of abundance (in longitude or latitude) as a response variable, and  
 631 survey year as the explanatory variable. Black bars indicate the 95% confidence intervals of  
 632 temporal slopes. Differences in the rate of change between body size groups were visualized using  
 633 loess regression prediction (blue line) and 95% confidence intervals (grey shade), including the  
 634 temporal slope of body size groups as the response variable and body size group as the continuous  
 635 explanatory variable. Size-dependent effects of sea bottom temperature (Temperature) and total  
 636 stock biomass (Biomass) on the area of distribution and the center of abundance were examined in  
 637 linear regression, by including interaction terms of Temperature or Biomass with body size group

638 in the initial models (further details in Methods). Significant explanatory variables ( $p < 0.05$ ) from  
639 the most parsimonious models are shown, with positive effects (+), negative effects (-), or size-  
640 dependent effect ( $\times$  body size).



643 **Fig. 5 Conceptual diagram illustrating changes in overlapped area between body size groups**  
 644 **within populations in response to ocean warming and population biomass decline.** Circle  
 645 represents the theoretical area of distribution of smaller (red) or larger groups (blue) within each  
 646 population in a two-dimensional space. Black dots indicate centers of abundance. The direction of  
 647 arrows in red or blue indicate expansion (outward) or contraction (inward) of the area of distribution  
 648 for large or small groups, respectively, and the thickness of arrows indicates the magnitude of  
 649 change. Black arrow indicates the direction of shift in the center of abundance. Changes in the area  
 650 of distribution and center of abundance may or may not occur chronologically.